Structure, Volume *23*

Supplemental Information

Structural Basis of Latrophilin-FLRT-UNC5 Interaction in Cell Adhesion

Yue C. Lu, Olha V. Nazarko, Richard Sando, III, Gabriel S. Salzman, Nan-Sheng Li, Thomas C. Südhof, and Demet Araç

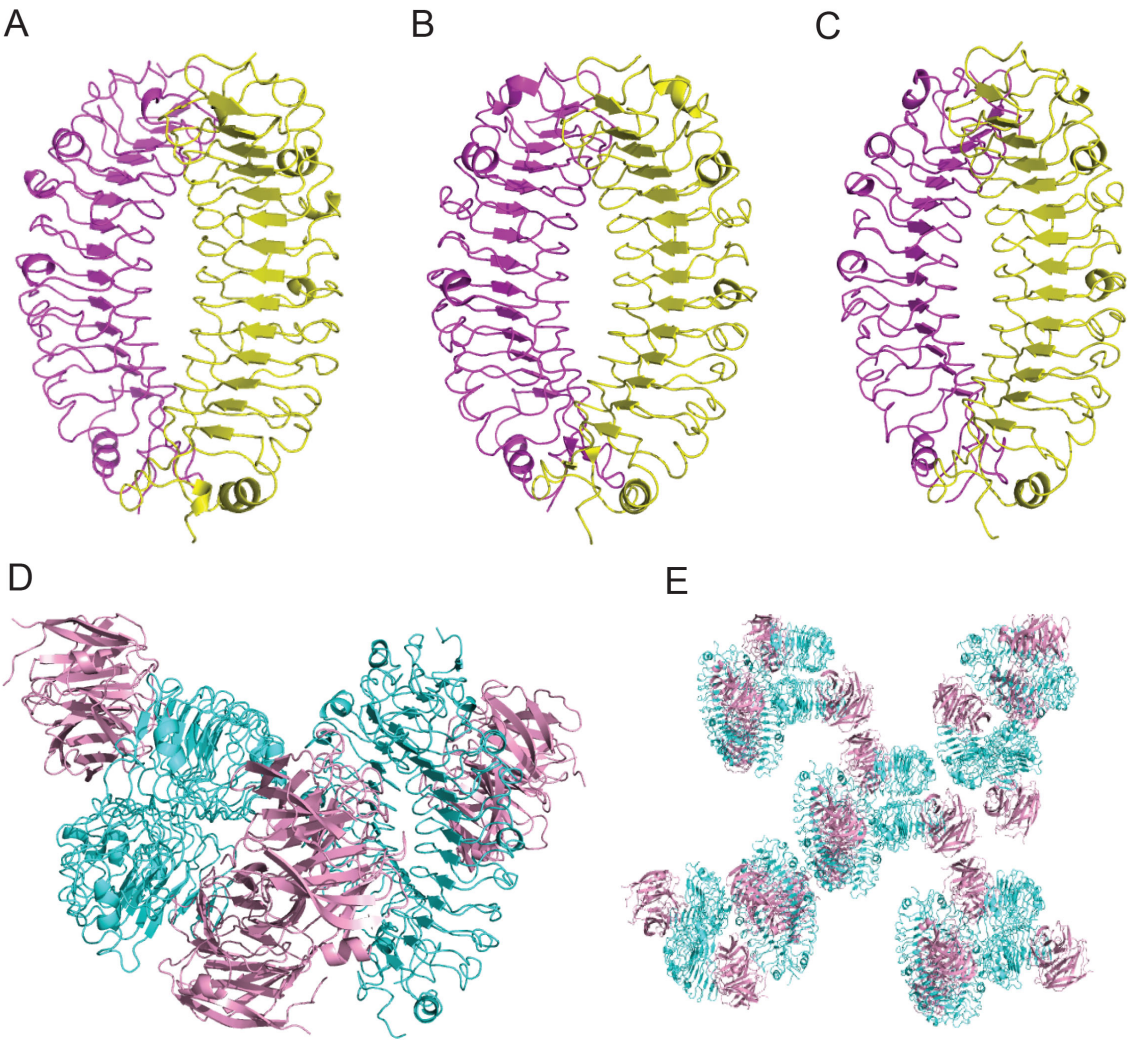
A
B
C
D
E

Figure S1, related to Figure 1

Crystal structure of the isolated FLRT3 LRR, and the crystal lattice of the FLRT3/LPHN3 complex structure.

(A) Ribbon diagram of the isolated human FLRT3 LRR in $P2_1$ space group. Two FLRT3 molecules make an interface on the side surface of FLRT3 where UNc5 binds. The previously reported mouse FLRT3 LRR dimer interface does not exist in our new isolated human FLRT3 structure. (B) Ribbon diagram of the published mouse FLRT3 LRR structure (PDB ID: 4V2E) showing the same interface as in A exists in both isolated FLRT3 structures. (C) Ribbon diagram of the FLRT3/LPHN3 complex structure showing only the FLRT3 LRR. Figure shows the same interface as in A and B also exists in the FLRT3/LPHN3 complex structure. The previously reported FLRT3 LRR dimer interface does not exist in the FLRT3/LPHN3 complex structure. These observations suggest that the observed interface in A,B and C can indeed be the dimer interface. It is also likely that the observed interface is a crystallization artifact that is preferred to generate crystal contacts. Careful mutagenesis experiments will answer these questions. (D) Ribbon diagram showing four FLRT3/LPHN3 complexes in the asymmetric unit of the complex structure. (E) A view of the FLRT3/LPHN3 complex structure crystal lattice.

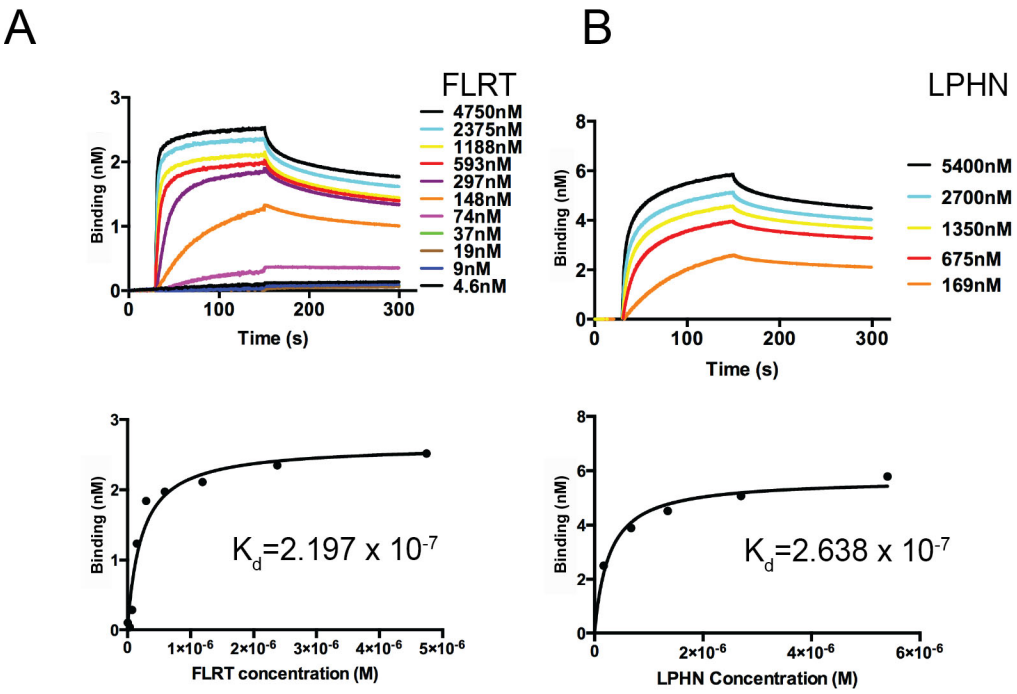

Figure S2, related to Figure 2

Bio-layer interferometry binding measurement of FLRT3 and LPHN3.

LPHN3 and FLRT3 bind to each other in the nanomolar range. Maximum binding of His-tagged FLRT3 LRR to immobilized biotinylaed LPHN3 Olf (A), or His-tagged LPHN3 to immobilized biotinylated FLRT3 LRR (B), measured at steady state during immersion of streptavidin sensor immobilized with biotinylated FLRT3 LRR or bitinylated LPHN3 Olf into various concentrations of His-LPHN3 Olf or His-FLRT3 LRR, respectively. Binding signal was plotted as a function of His-FLRT3 LRR or His-LPHN3 Olf concentration. The dissociation constants were calculated by fitting the curves to a single site binding model using GraphPad Prism.

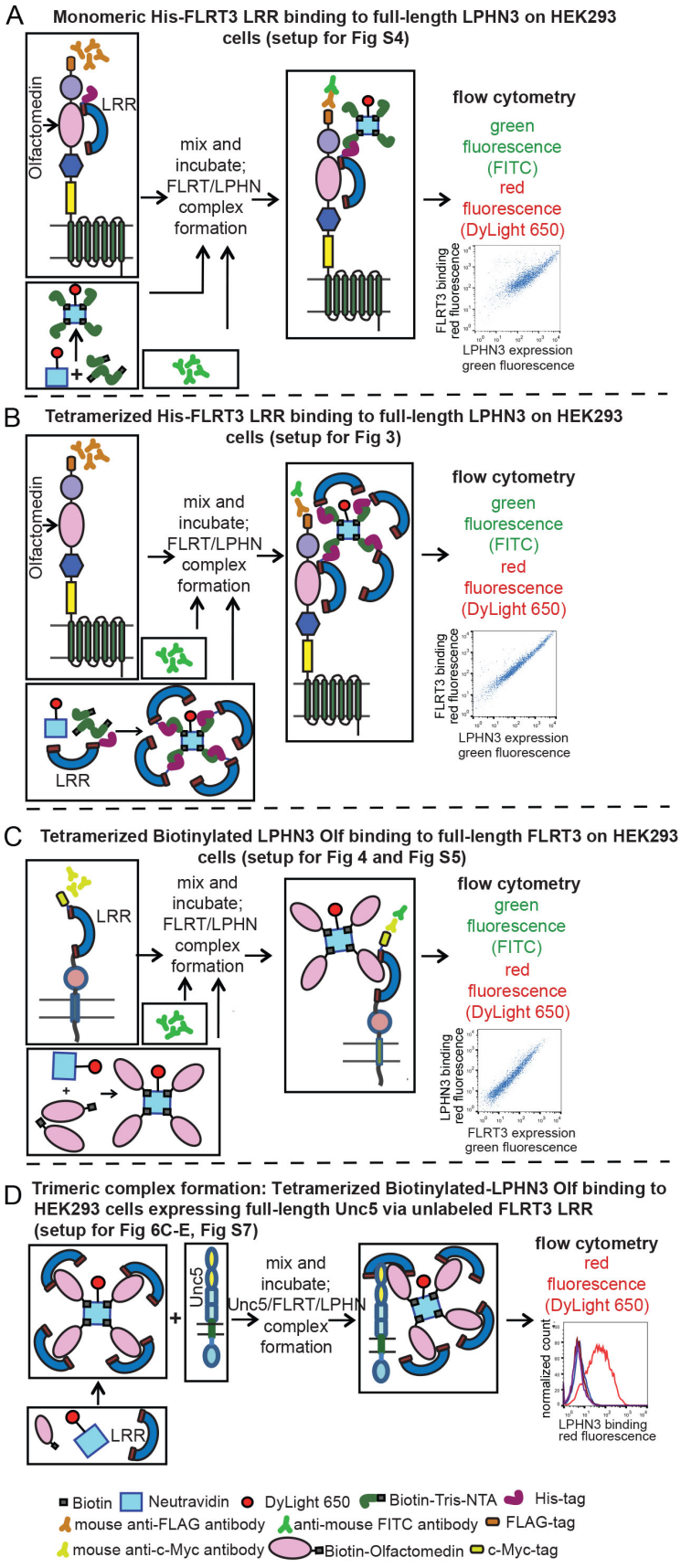
A
Monomeric His-FLRT3 LRR binding to full-length LPHN3 on HEK293 cells (setup for Fig S4)
Olfactomedin
LRR
mix and incubate; FLRT/LPHN complex formation
flow cytometry
green fluorescence (FITC)
red fluorescence (DyLight 650)
FLRT3 binding red fluorescence
LPHN3 expression green fluorescence
B
Tetramerized His-FLRT3 LRR binding to full-length LPHN3 on HEK293 cells (setup for Fig 3)
Olfactomedin
mix and incubate; FLRT/LPHN complex formation
flow cytometry
green fluorescence (FITC)
red fluorescence (DyLight 650)
FLRT3 binding red fluorescence
LPHN3 expression green fluorescence
LRR
C
Tetramerized Biotinylated LPHN3 Olf binding to full-length FLRT3 on HEK293 cells (setup for Fig 4 and Fig S5)
LRR
mix and incubate; FLRT/LPHN complex formation
flow cytometry
green fluorescence (FITC)
red fluorescence (DyLight 650)
LPHN3 binding red fluorescence
FLRT3 expression green fluorescence
D
Trimeric complex formation: Tetramerized Biotinylated-LPHN3 Olf binding to HEK293 cells expressing full-length Unc5 via unlabeled FLRT3 LRR (setup for Fig 6C-E, Fig S7)
Unc5
mix and incubate; Unc5/FLRT/LPHN complex formation
flow cytometry
red fluorescence (DyLight 650)
normalized count
LPHN3 binding red fluorescence
LRR
Biotin
Neutravidin
DyLight 650
Biotin-Tris-NTA
His-tag
mouse anti-FLAG antibody
anti-mouse FITC antibody
FLAG-tag
mouse anti-c-Myc antibody
Biotin-Olfactomedin
c-Myc-tag

Figure S3, related to Figure 3,4 and 6

Experimental Setup for Flow Cytometry experiments

N-terminally tagged full-length proteins (Flag-LPHN3, Myc-FLRT3, His-Unc5D or His-Unc5B) were expressed in HEK293 cells. Cells were then mixed wirh different combinations of soluble proteins and reagents before performing flow cytometry experiements. Black boxes around proteins or reagents indicate they were pre-incubated before mixing with the other components. Neutravidin is a tetrameric protein with four biotin-binding sites and was used to tetramerize the biotinylated proteins to increase the affinity of the protein due to the avidity effect. Biotin-Tris-NTA is a reagent (kindly provided by the S. Koide lab) to convert His-tagged soluble proteins to biotinylated proteins (It was used when expression/purification of biotinylated proteins was not optimal). Detection of full-length protein expression on the cell surface was monitored by green fluorescence of FITC-conjugated secondary anti-mouse antibody by flow cytometry. Monomeric or tetramerized soluble protein binding to the cells was monitored by red fluorescence of DyLight-conjugated neutravidin by flow cytometry.

(A) Setup in Figure S4. Monomeric His-FLRT3 LRR binding to HEK293 cells expressing full-length wild type or mutant LPHN3. Biotin-Tris-NTA was used to recognize His tagged FLRT3 LRR.

(B) Setup in Figure 3. Tetramerized His-FLRT3 LRR binding to HEK293 cells expressing full-length wild type or mutant LPHN3. His-FLRT3 LRR is tetrametrized by preincubation with Neutravidin and Biotin-Tris-NTA.

(C) Setup in Figure 4 and S5. Tetramerized biotinylated-LPHN3 olf binding to HEK293 cells expressing full-length wild-type or mutant FLRT3. Biotin-tagged LPHN3 Olf was first biotinylated by in vitro biotibyation. Biotinylated LPHN3 Olf is tetrametrized by preincubation with Neutravidin.

(D) Setup for Figure 6 and S7. Tetramerized biotinylated-LPHN3 Olf binding to HEK293 cells expressing full-length wild-type Unc5D or Unc5B. Biotinylated LPHN3 Olf and non-biotinylated His-tagged FLRT3 LRR is tetrametrized by preincubation with Neutravidin. The formation of a trimeric complex of His-FLRT3 LLR, biotinylated LPHN3 olf domain and FL-Unc5 expressed by HEK293 cells is observed.

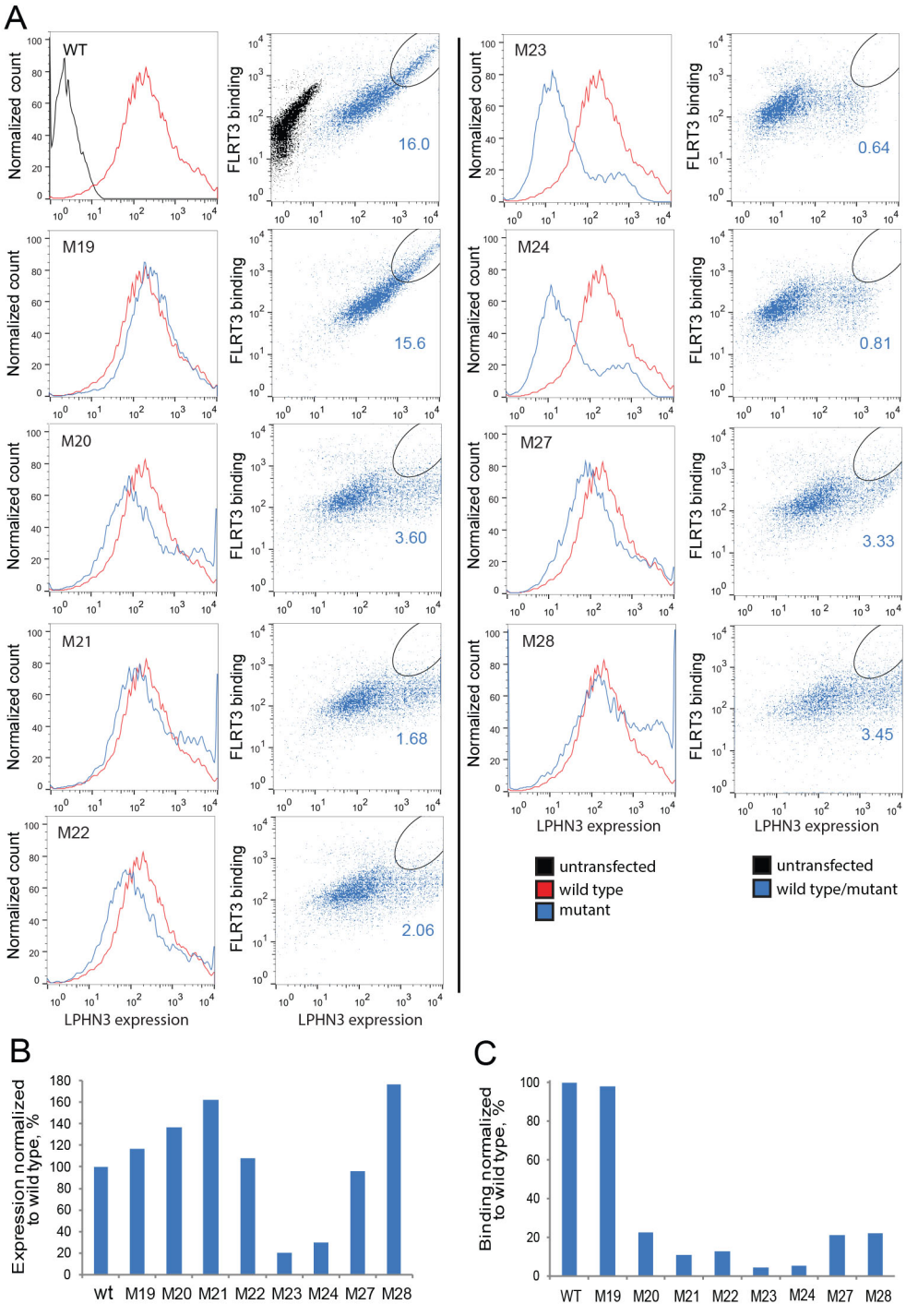
A
WT
M19
M20
M21
M22
M23
M24
M27
M28
Normalized count
FLRT3 binding
LPHN3 expression
16.0
15.6
3.60
1.68
2.06
0.64
0.81
3.33
3.45
untransfected
wild type
mutant
untransfected
wild type/mutant

B
Expression normalized to wild type, %
wt
M19
M20
M21
M22
M23
M24
M27
M28

C
Binding normalized to wild type, %
WT
M19
M20
M21
M22
M23
M24
M27
M28

Figure S4, related to Figure 3

Expression and FLRT3 LRR-binding data for all FL-LPHN3 mutants

Wild-type and mutant full-length LPHN3 constructs were tested for surface expression in non-permeabilized HEK293 cells as well as their ability to bind to soluble His-FLRT3 LRR domain using flow cytometry

(A) FL-LPHN3 surface expression in wild-type FL-LPHN3-transfected cells (red) compared to untransfected cells (black), and to mutant FL-LPHN3-transfected cells (blue) (left panels). Non-permeabilized HEK293 cells expressing N-terminally FLAG-tagged FL-Lphn3 were stained with mouse anti-FLAG primary antibody and anti-mouse FITC conjugated secondary antibody. FL-LPHN3 surface expression was measured as green fluorescence from FITC. His-FLRT3 LRR binding to FL-LPHN3-expressing cells was measured by monitoring red fluorescence of DyLight attached to neutravidin (y-axis, right panles). 10 μM non-tetramerized His-FLRT3 LRR was mixed with the cells, then 100 nM Biotin-Tris-NTA and 100 nM Neutravidin was added for detection of His-FLRT3 LRR binding. Black ovals show the “high LPHN3 expression and high FLRT3 binding” gate. Numbers on the dot plot show percent of events in this gate. (Refer to Figure S3 and Table S3 for detailed experimental setup and experimental conditions)

(B) Surface expression of mutant LPHN3 transfected cells normalized to wild type.

(C) Quantification of cells that fall within the gate of “high LPHN3 expression and high FLRT3 binding” (black ovals) as indicated in A. Bar height represents the percent of cells that fall within the gates shown.

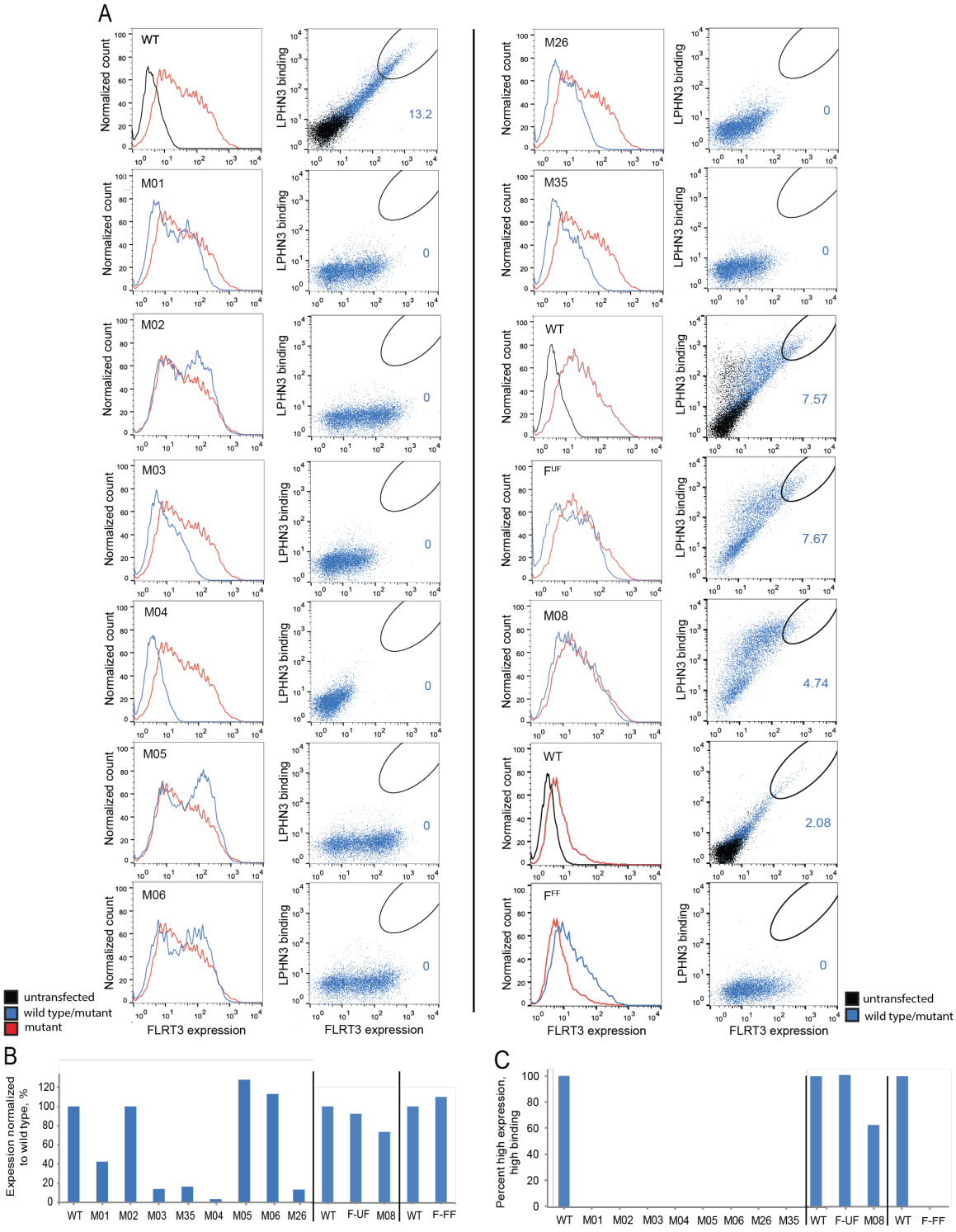
A
WT
M01
M02
M03
M04
M05
M06
M26
M35
WT
F^UF
M08
WT
F^FF
Normalized count
LPHN3 binding
13.2
0
0
0
0
0
0
0
7.57
7.67
4.74
2.08
0
FLRT3 expression
FLRT3 expression
FLRT3 expression
FLRT3 expression
untransfected
wild type/mutant
mutant
untransfected
wild type/mutant
B
Expression normalized to wild type, %
WT M01 M02 M03 M35 M04 M05 M06 M26 WT F-UF M08 WT F-FF
C
Percent high expression, high binding
WT M01 M02 M03 M04 M05 M06 M26 M35 WT F-UF M08 WT F-FF

Figure S5, related to Figure 4

Expression and LPHN3 Olf-binding data for all FL-FLRT3 mutants

Wild-type and mutant full-length FLRT3 constructs were tested for surface expression in non-permeabilized HEK293 cells as well as their ability to bind to soluble biotinylated LPHN3 Olf domain using flow cytometry

(A) FL-FLRT3 surface expression in wild-type FL-FLRT3-transfected cells (red) compared to untransfected cells (black), and to mutant FL-FLRT3-transfected cells (blue) (left panels). Non-permeabilized HEK293 cells expressing N-terminally Myc-tagged FL-FLRT3 were stained with mouse anti-c-Myc primary antibody and anti-mouse FITC conjugated secondary antibody. FL- FLRT3 surface expression was measured as green fluorescence from FITC. Biotinylated LPHN3 Olf binding to FL- FLRT3-expressing cells was measured by monitoring red fluorescence of DyLight attached to neutravidin (y-axis, right panles). 100nM purified wild-type biotinylated LPHN3 Olf domain was tetramerized with 100 nM Neutravidin to increase avidity before binding to cells. Black ovals show the “high FLRT3 expression and high LPHN3 binding” gate. Numbers on the dot plot show percent of events in this gate. (Refer to Figure S3 and Table S3 for detailed experimental setup and experimental conditions)

(B) Surface expression of mutant FLRT3 transfected cells normalized to wild type.

(C) Quantification of cells that fall within the gate of “high FLRT3 expression and high LPHN3 binding” (black ovals) as indicated in A. Bar height represents the percent of cells that fall within the gates shown. Separate sets of experiments are indicated by vertical lines. Wild type data is provided as positive control for each dataset.

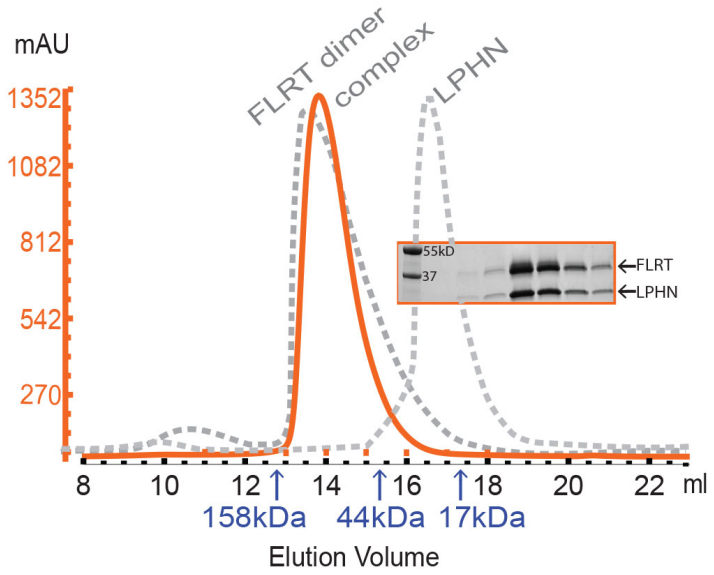

Figure S6, related to Figure 5

Size-exclusion gel filtration profile showing the formation of FLRT3/LPHN3 complex. Dotted lines represent FLRT LRR dimer and LPHN3 Olf for reference. SDS-Page gel shows fractions corresponding to the complex peak. The elution volumes and corresponding molecular weights for the gel filtration standards are indicated by blue arrows.

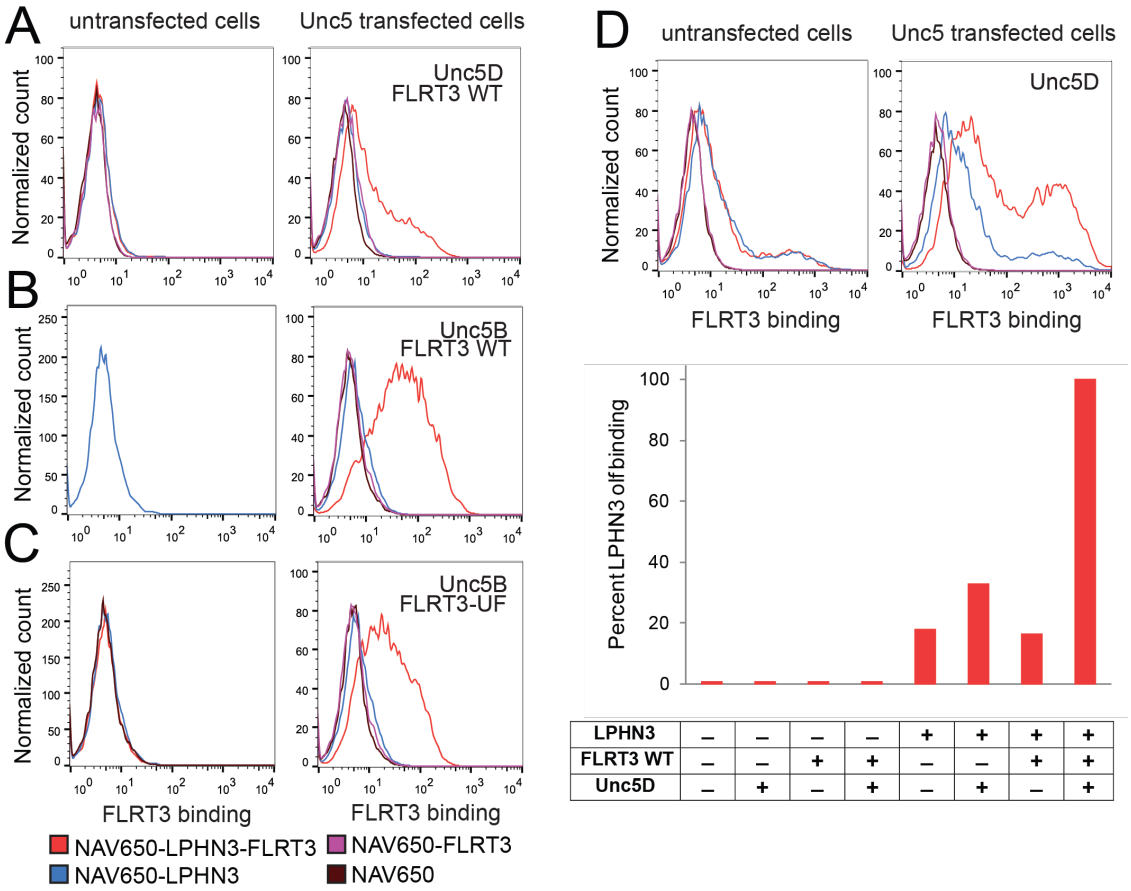

Figure S7, related to Figure 6

Formation of a trimeric complex between FLRT3, LPHN3 and Unc5

(A to C) Raw data for Figure 6C to E. Untrasfected HEK293 cells or cells transfected with Unc5 were stained with a precomplex of biotinylated LPHN3 Olf domain, unlabeled His-FLRT3 LRR and neutravidin (NAV650) in different combinations to detect binding of LPHN3 Olf to cells with flow cytometry. Unc5D or Unc5B transfected HEK293 cells were tested for binding with 100 nM LPHN3 olf and wild type FLRT3, or LPHN3 Olf and FLRT-UF mutant precomplex. Panel A data was performed with 5 nM protein concentration with tetramerization, whereas panels B and C were performed with 100 nM protein concentration. Panel A was repeated with 100 nM protein concentration with tetramerization as shown in (D). Similar results were obtained but some non-specific binding is observed when 100 nM concentration was used. See Figure S3 and Table S3 for details about experimental setup and conditions.

```
Conservation:                          7 7  6                9 9  9            6  6         6 77     7
human_Lphn3                 131 -KVFLCPGLLKGVYQSEHLFESD---HQSGAWCKDPLQAS----DKIYYMPWTPYRTDTLTEYSSKDDFI
rat_Lphn1                   137 --VFVCPGTLQKVLEPTSTHESE---HQSGAWCKDPLQAG----DRIYVMPWIPYRTDTLTEYASWEDYV
human_Lphn2                 133 --IFVCPGTLKAIVDSPCIYEAE---QKAGAWCKDPLQAA----DKIYFMPWTPYRTDTLIEYASLEDFQ
danio rerio_Lphn3.1         190 ------------------------------------------------MPWTPYRTDTLTEYSSKEDFI
myotis lucifugus_Lphn3        4 --VFLCPGLLKGVYQSEHLFESD---HQSGAWCKDPLQAS----DKIYYMPWTPYRTDTLTEYSSKDDFI
pelodiscus sinensis_Lphn3     1 --VFLCPGLLKGVYQSEHLFESD---HQSGAWCKDPLQAS----DKIYYMPWTPYRTDTLTEYSSKDDFI
human_Myoc                  239 GEGDTGCGELVWVGEPLTLRTAETITGKYGVWMRDPKPTYPYTQETTWRIDTVGTDVRQVFEYDLISQFM
macaque_Myoc                226 REGDNGCGELVWVGEPLTLRTAETITGKYGVWMRDPKPTYPYTRETTWRIDTVGTDVRQVFEYDLISQFM
xenopus laevis_Olfml3       129 --ITDCSDTISQVTAMKILKRFG---SSAGLWTKDLAGNS----DRIYVFDGAG--NDTVYMYPRMKEFT
human_Noelin-1_             221 CMQKLACGKLTGISDPVTVKTSG---SRFGSWMTDPLAPEG--DNRVWYMDGY-HNNRFVREYKSMVDFM
human_Noelin-2              189 CAQKLGCGKLTGVSNPITVRAMG---SRFGSWMTDTMAPSA--DSRVWYMDGY-YKGRRVLEFRTLGDFI
rat_Noelin-3                213 CMKKLTCGKLMKITGPITVKTSG---TRFGAWMTDPLASEK--NNRVWYMDSY-TNNKIVREYKSIADFV
Consensus_ss:                         eeeee   eeeeee         eee           eeeee        eeeee  hhhhh

Conservation:                                99    797 799 9  66        6666 6          6  766     9 77
human_Lphn3                 AGR---PTTTYKLPHRVDGTGFVVYDGALFFNKER-TRNIVKFDLRTRIKSGEAIIANANYHDTSPYRWG
rat_Lphn1                   AAR---HTTTYRLPNRVDGTGFVVYDGAVFYNKER-TRNIVKYDLRTRIKSGETVINTANYHDTSPYRWG
human_Lphn2                 NSR---QTTTYKLPNRVDGTGFVVYDGAVFFNKER-TRNIVKFDLRTRIKSGEAIINYANYHDTSPYRWG
danio rerio_Lphn3.1         AGR---PTTTYKLPHRVDGTGFVVYDGALFFNKER-TRNIVKFDLRTRIKSGEAIIANANYHDTSPYRWG
myotic lucifugus_Lphn3      AGR---PTTTYKLPHRVDGTGFVVYDGALFFNKER-TRNIVKFDLRTRIKSGEAIIANANYHDTSPYRWG
pelodiscus sinensis_Lphn3   AGR---PTTTYKLPHRVDGTGFVVYDGALFFNKER-TRNIVKFDLRTRIKSGEAIIANANYHDTSPYRWG
human_Myoc                  QGY---PSKVHILPRPLESTGAVVYSGSLYFQGAE-SRTVIRYELNTETVKAEKEIPGAGYHGQFPYSWG
macaque_Myoc                QGY---PSKVHILPRPLESTGAVVYSGNLYFQGAE-SRTVIRYELNTETVKAQKEIPGAGYHGQFPYSWG
xenopus laevis_Olfml3       LSSPTRKAAKIRLPFPWIGTGHIVYDGNLYYIRQDNEFQVIKFSLANKTIIDSAVLPIE--QQVPVYGLS
human_Noelin-1              NTD---NFTSHRLPHPWSGTGQVVYNGSIYFNKFQ-SHIIIRFDLKTETILKTRSLDYAGYNNMYHYAWG
human_Noelin-2              KGQ---NFIQHLLPQPWAGTGHVVYNGSLFYNKYQ-SNVVVKYHFRSRSVLVQRSLPGAGYNNTFPYSWG
rat_Noelin-3                SGA---ESRTYNLPFKWAGTNHVVYNGSLYFNKYQ-SNIIIKYSFDLGRVLAQRSLEYAGFHNVYPYTWG
Consensus_ss:               h       eeee         eeeee eeeee       eeeee    eeeeeeee          ee

Conservation:               7  779  699 99966959  7 7 77 7 967  9     9 9   7 57  79 699 997
human_Lphn3                 GKSDIDLAVDENGLWVIYATEQNNGKIVISQLNPYTLRIEGTWDTAYDKRSASNAFMICGILYVVKSVYE
rat_Lphn1                   GKTDIDLAVDENGLWVIYATEGNNGRLVVSQLNPYTLRFEGTWETGYDKRSASNAFMVCGVLYVLRSVYV
human_Lphn2                 GKTDIDLAVDENGLWVIYATEQNNGMIVISQLNPYTLRFEATWETVYDKRAASNAFMICGVLYVVRSVYQ
danio rerio_Lphn3.1         GKSDIDLAVDENGLWVIYATEQNNGRIVVSQLNPYTLRVEGSWDTSYDKRSASNAFMICGILYVVKSVYE
myotis lucifugus_Lphn3      GKSDIDLAVDENGLWVIYATEQNNGKIVISQLNPYTLRIEGTWDTAYDKRSASNAFMICGILYVVKSVYE
pelodiscus sinensis_Lphn3   GKSDIDLAVDENGLWVIYATEQNNGKIVISQLNPYTLRIEGTWDTAYDKRSASNAFMICGILYVVKSVYE
human_Myoc                  GYTDIDLAVDEAGLWVIYSTDEAKGAIVLSKLNPENLELEQTWETNIRKQSAANAFIICGTLYTVSSYT-
macaque_Myoc                GYTDIDLAVDESGLWVIYSTDEAKGAIVLSKLNPENLELEQTWETNIRKQSAANAFIICGTLYTVSSYS-
xenopus laevis_Olfml3       KFNYIDIVADEEGLWVIYATKENEKNICLAKLDPSSLSIEQMWDTPCPIENAESAFVVCGSLYVVYNTKL
human_Noelin-1              GHSDIDLMVDESGLWAVYATNQNAGNIVVSRLDPVSLQTLQTWNTSYPKRSAGEAFIICGTLYVTNGYS-
human_Noelin-2              GFSDMDFMVDESGLWAVYTTNQNAGNIVVSRLDPHTLEVMRSWDTGYPKRSAGEAFMICGVLYVTNSHL-
rat_Noelin-3                GFSDIDLMADEIGLWAVYATNQNAGNIVISQLNQDTLEVMKSWSTGYPKRSAGEAFMICGTLYVTNSHL-
Consensus_ss:                   eeeeee   eeeeee      eeeeeee     eeeeeee       hhheeeeeeeeeeee

Conservation:                            6   6 7             9 7 9   6  7997 6  77 967     7       6
human_Lphn3                 DDDNEATGNKIDYIYNTDQ--SKDSLVDVPFPNSYQYIAAVDYNPRDNLLYVWNNYHVVKYSLDFGPLDS 396
rat_Lphn1                   DDDSEAAGNRVDYAFNTNA--NREEPVSLAFPNPYQFVSSVDYNPRDNQLYVWNNYFVVRYSLEFGPPDP 401
human_Lphn2                 DNESETGKNSIDYIYNTRL--NRGEYVDVPFPNQYQYIAAVDYNPRDNQLYVWNNNFILRYSLEFGPPDP 397
danio rerio_Lphn3.1         DDDNEALGNKIDYMYNTEK--SRETHLSIPFPNSYQYIAAVDYNPRDNLLYVWNNYHVVIYSLDFGNNDN 414
myotis lucifugus_Lphn3      DDDNEATGNKIDYIYNTDQ--SKDSVVDVPFPNSYQYIAAVDYNPRDNLLYVWNNYHVVKYSLDFGPLDS 268
pelodiscus sinensis_Lphn3   DDDNEATGNKIDYIYNTDQ--SKDSLVDVPFPNSYQYIAAVDYNPRDNLLYVWNNYHVVKYSLDFGPLDS 286
human_Myoc                  -----SADATVNFAYDTGT--GISKTLTIPFKNRYKYSSMIDYNPLEKKLFAWDNLNMVTYDIKLSKM-- 504
macaque_Myoc                -----SADATVNFAYDTGT--GISKTLTIPFKNRYKYSSMIDYNPLEKKLFAWDNLNMVTYDIKLSKM-- 491
xenopus laevis_Olfml3       -----PSRSRIQCVFDVSGTISSENVPIVYFPKRYGSHSSMKYNPREKQIYAWDDGYQIIYKLNMKHRDE 390
human_Noelin-1              ------GGTKVHYAYQTNA--STYEYIDIPFQNKYSHISMLDYNPKDRALYAWNNGHQILYNVTLFHVIR 481
human_Noelin-2              ------AGAKVYFAYFTNT--SSYEYTDVPFHNQYSHISMLDYNPRERALYTWNNGHQVLYNVTLFHVIS 449
rat_Noelin-3                ------TGAKVYYSYSTKT--STYEYTDIPFHNQYFHISMLDYNARDRALYAWNNGHQVLFNVTLFHIIK 473
Consensus_ss:                        eeeeeee       eee            eeee  hhh eeeeee  eeeeeeeee
```

Table S1, related to Figure 2

Sequence alignment of Olfactomedin domains

Sequence alignment of olfatomedin domains using PROMALS3D: human LPHN3 (Uniprot ID: Q9HAR2), rat LPHN1 (O88917), human LPHN2 (O95490), *daniorerio* LPHN3.1 (F1QAS7), *myotislucifugus* LPHN3 (G1P220), *pelodiscussinensis* LPHN3 (K7F4U8), human Myocilin (Q99972), *macacafascicularis*Myocilin (Q863A3), *xenopuslaevis* Olfml3 (B5MFE9), human Noelin1 (Q99784), human Noelin2 (O95897), rat Noelin2 (Q568Y7). The first line in each block shows conservation indices with 9 being the most conserved and 7 and 6 being less conserved. Consensus predicated secondary structures are represented by *h*, alpha-helix, or *e*, beta-strand.

```
Conservation:                    6       9                      99969999  9699969 99969 699 6696969
human_FLRT3              1  -----MISAAWSIFLIGTKIGLFLQVAPLSVMAKSCPSVCRCDAGFIYCNDRFLTSIPTGIPEDATTLYL
human_FLRT1              1  -----MDLRDW-LFLCYGLIAFLTEV----IDSTTCPSVCRCDNGFIYCNDRGLTSIPADIPDDATTLYL
human_FLRT2              1  MGLQTTKWPSHGAFFLKSWLIISLGLYSQVSKLLACPSVCRCDRNFVYCNERSLTSVPLGIPEGVTVLYL
danio rerio_FLRT3        1  -----MASNYMSFFVFFIRAGLLLGLANPLMTSASCPSQCRCDGTFIYCNDRDLTSIPSGIPEDATVLFL
xenopus laevis_FLRT3     1  -----MSTETWNLFVAWAQLLLLFRISPQYVNAKPCPSVCRCDGGFIYCNDRDLTSIPSGIPDDATTLYL
Consensus_ss:                         hhhhhhhhhhhhhhhhhh           ee   eee                  eee


Conservation:                69969669969 69     9  6999 9 99999 999  666999969966699  6696 66 696999
human_FLRT3                  QNNQINNAGIPSDLKNLLKVERIYLYHNSLDEFPTNLPKYVKELHLQENNIRTITYDSLSKIPYLEELHL
human_FLRT1                  QNNQINNAGIPQDLKTKVNVQVIYLYENDLDEFPINLPRSLRELHLQDNNVRTIARDSLARIPLLEKLHL
human_FLRT2                  HNNQINNAGFPAELHNVQSVHTVYLYGNQLDEFPMNLPKNVRVLHLQENNIQTISRAALAQLLKLEELHL
danio rerio_FLRT3            QNNRIKSAGIPTDLRRLNGVEKIYLYCNNLDEFPTNLPLNVKELHLQENNIRTITHASLAQIPFIEELHL
xenopus laevis_Flrt3         QNNQINNAGIPSDLRGLDKVERIYLYRNSLDEFPINLPKNVKELHLQENNIRTITYDALSQIPSIEELHL
Consensus_ss:                           hhh      eee      eee         eee          hhhhhhhhhhhhee


Conservation:                99969669669669966   969999969999669 999 666999 969996 9   666 9 69 996
human_FLRT3                  DDNSVSAVSIEEGAFRDSNYLRLLFLSRNHLSTIPWGLPRTIEELRLDDNRISTISSPSLQGLTSLKRLV
human_FLRT1                  DDNSVSTVSIEEDAFADSKQLKLLFLSRNHLSSIPSGLPHTLEELRLDDNRISTIPLHAFKGLNSLRRLV
human_FLRT2                  DDNSISTVGVEDGAFREAISLKLLFLSKNHLSSVPVGLPVDLQELRVDENRIAVISDMAFQNLTSLERLI
danio rerio_FLRT3            DDNSVSAVSIEEGAFRDSNHLRLLFLSRNHLSTIPSGLPMTIEELRFDDNRISSISEASLQDLINLKRLV
xenopus laevis_FLRT3         DDNSVSAVSIEDGAFRDNIFLRLLFLSRNHLSTIPWGLPRTIEELRLDDNRISTIAEISLQDLTNLKRLV
Consensus_ss:                     ee      hh       eee                 eee          hhhh       eee


Conservation:                699999 9 6666  6  9 696969699999  69 6996  9 69 9969 6  69  666 66 969
human_FLRT3                  LDGNLLNNHGLGDKVFFNLVNLTELSLVRNSLTAAPVNLPGTNLRKLYLQDNHINRVPPNAFSYLRQLYR
human_FLRT1                  LDGNLLANQRIADDTFSRLQNLTELSLVRNSLAAPPLNLPSAHLQKLYLQDNAISHIPYNTLAKMRELER
human_FLRT2                  VDGNLLTNKGIAEGTFSHLTKLKEFSIVRNSLSHPPPDLPGTHLIRLYLQDNQINHIPLTAFSNLRKLER
danio rerio_FLRT3            LDGNLLNNRGIGEMALVNLVNLTELSLVRNSLTSPPANLPGSSLEKLNLQDNHINHVPPGAFAFLRQLYR
xenopus laevis_FLRT3         LDGNLLNNNGLGERVFMNLINLTELSLVRNSLTSPPANLPGTNLRKLYLQENHMNYVPPNAFADLTQLYR
Consensus_ss:                          hh       eee                   eee       ee hhhh       e


Conservation:                99 969 6  96 9 9669 96 69 699999 9 9  6966696   6  699996999696 969966
human_FLRT3                  LDMSNNNLSNLPQGIFDDLDNITQLILRNNPWYCGCKMKWVRDWLQSLPVKVNVRGLMCQAPEKVRGMAI
human_FLRT1                  LDLSNNNLTTLPRGLFDDLGNLAQLLLRNNPWFCGCNLMWLRDWVKARAAVVNVRGLMCQGPEKVRGMAI
human_FLRT2                  LDISNNQLRMLTQGVFDNLSNLKQLTARNNPWFCDCSIKWVTEWLKYIPSSLNVRGFMCQGPEQVRGMAV
danio rerio_FLRT3            LDLSGNNLSSLPMGVFEDLDNLTQLLLRNNPWHCNCRMKWVRDWLRTLPSKVNVRGFMCQGPDKVKGMAI
xenopus laevis_FLRT3         LDMSNNNITALPQGIFDDLDNLTQLFLRNNPWYCGCKMKWVRDWLQSLPSKVNVRGLMCQAPERVRGMTI
Consensus_ss:                ee          hhhhh      eee           hhhhhhhhhh          ee   hhh   ee


Conservation:                666  66  9                   6   9           6  6  666 6    96
human_FLRT3                  KDLNAELFDCKDSG-------------IVSTIQITTAIPNTVYPAQGQWPAPVTKQPDIKNPKLTKDHQT 402
human_FLRT1                  KDITSEMDECFETGPQGGV--------ANAAAKTTASNHASATTPQGSLFTLKAKRPGLRLPDSNIDYPM 402
human_FLRT2                  RELNMNLLSCPTTTPGLPLFTPAPSTASPTTQPPTLSIPNPSRSYTPPTP---TTSKLPTIPDWDGRERV 417
danio rerio_FLRT3            KDLSTELFGCSDTE-------------IPTTYE-TSTVSNTLPPSRPQWPSYVTKRPVVKGPDLGRNYRS 401
xenopus laevis_FLRT3         KDLNKELFDCKDRI-------------GSNTIHVTTTVLNSLLPAQGQWPVPVTKQPEIRPPDINKIFRT 402
Consensus_ss:                ee  hhh                     eee                ee
```

Table S2, related to Figure 2

Sequence alignment of LRR repeats of FLRT homologs

Sequence alignment of FLRT3 LRR domains using PROMALS3D: human FLRT3 (Uniprot ID: Q9NZU0), *xenopus laevis* (B7ZR53), *danio rerior* (B8A507), human FLRT2 (O43155), and human FLRT1 (Q9NZU1). The first line in each block shows conservation indices with 9 being the most conserved and 7 and 6 being less conserved. Consensus predicated secondary structures are represented by h, alpha-helix, or e, beta-strand.

Experiment purpose	**Scheme**	**Data**	**Reagents used**				
Cell-surface expression			**primary antibody**		**secondary antibody**		**Fluorophore**
FLAG-LPHN3 full length	-	**Fig 3, S4**	mouse anti-FLAG 1:1000		anti-mouse FITC 1:100		FITC
Myc-FLRT3 full length	-	**Fig 4, S5**	mouse anti-c-Myc 1:20		anti-mouse FITC 1:100		FITC
Detect soluble protein binding to cells			**neutravidin DyLight 650**	**biotin-tris-NTA**	**Biotinylated-LPHN3 Olf**	**His-FLRT3 LRR**	
monomeric His-FLRT3 LRR	**Fig S3A**	**Fig S4**	100 nM	100 nM	**-**	10 µM	DyLight 650
tetramerized His-FLRT3 LRR	**Fig S3B**	**Fig 3**	100 nM	100 nM	**-**	100 nM	DyLight 650
tetramerized Biotinylated-LPHN3	**Fig S3C**	**Fig 4; Fig S5**	100 nM	**-**	100 nM	**-**	DyLight 650
Trimeric complex Unc5/FLRT3/LPHN3	**Fig S3D**	**Fig 6C, S7A/ Fig 6D-E, S7B-D**	5 nM/ 100 nM	**-**	5 nM/ 100 nM	5 nM/ 100 nM	DyLight 650

Table S3. Related to Figures 3,4,6,S3,S4,S5,S7. Summary of experimental conditions for flow cytometry.

Table showing experimental conditions used for performing the flow cytometry experiments in the related figures. Experimental conditions for both detecting cell-surface expression and for detecting soluble protein binding to surface expressed proteins are summarized. The schematic diagram explaining the experiment and the data related to the experiment are indicated in separate columns.

Supplementary Methods

Vector and Cloning

For crystallization and protein purification, the LRR repeats of human FLRT3 (residues K29-D357; Uniprot ID: Q9NZU0) was cloned into the XmaI and Not I sites of the pAcGP67a. The olfactomedin domain of human LPHN3 (residues V132-G392; Uniprot ID: Q9HAR2) was cloned into the BamHI and XbaI sites of pAcGP67a. Similarly, the Ig-like domain of mouse Unc5D (residues G49-Q161; Uniprot ID: Q6UXZ4) was cloned into BamHI and NotI sites of pAcGP67a. A His8 tag or biotin tag was added at the C terminus for affinity purification. For mammalian expression and functional analysis, full length human FLRT3 (residues S30-S649), human LPHN3 (residues F20-L1447), and human Unc5B (G27-E934; Uniprot ID: Q8IZJ1), and mouse Unc5D (S46-L884) constructs with preprotrypsin leader sequence containing N-terminal myc, FLAG, His and His-tags, respectively, were cloned into pCMV5 plasmid using Gibson Assembly (NEB). Site directed mutagenesis for FLRT3 and LPHN3 mutants was performed using the Qiagen QuikChange Mutagenesis (QIAGEN).

Protein Expression and Purification

Spodoptera frugiperda (Sf9) cells (Life Technologies) were transfected with pAcGP67a carrying the gene and linearized baculovirus DNA (BestBac 2.0, v-cath/chiA deleted; Expression Systems) using Cellfectin (Life Technologies). Baculovirus was amplified in Sf9cells in 10%(v/v) fetal bovine serum containing SF900-II SFM medium (Life Technologies).

Large-scale protein expression was performed by infection of *Tri choplusiani* (Hi5) cells in Insect-Xpress medium (Lonza) at a cell density of 2×10^6cells/ml with an infection course of 72hr. The secreted, glycosylated recombinant proteins were purified using nickel-nitrilotriacetic agarose resin (QIAGEN) and size exclusion chromatography (Superdex 200 10/300 GL; GE) in HBS buffer (10mM HEPES (pH7.2), 150mM NaCl). FLRT was concentrated to 15mg/ml in 10kDa Centricon (Millipore) at 12°C and used for crystallization trials. It was observed that FLRT at high concentration tends to precipitate at 4° C, displaying a white cloudy color. However, precipitation was reversible when concentrated FLRT was warmed up to room temperature.

For FLRT/LPHN3 complex crystallization, purified FLRT and LPHN3 were mixed at 1:1.2 ratio. The complex was purified by size-exclusion chromatography in buffer containing 10mM HEPES (pH7.2), 150 mM NaCl and concentrated to 20 mg/ml in 10 kDa Centricon (Millipore) at 12°C.

For BLITZ and some flow cytometry experiments FLRT3 LRR and LPHN3 Olf were cloned into a pACGP67a vector that carries a C-terminal Avi-tag (sequence GLNDIFEAQKIEWHE) followed by a 6XHis tag. The purified Avi-tagged proteins were biotinylated *in vitro* with purified BirA enzyme that recognizes the Avi-tag and biotinylates it.

Crystallization, Data Collection, and Processing

Prior to crystallization, purified proteins were incubated with carboxypeptidase A (1:100 enzyme to protein ratio; Sigma-Aldrich) and carboxypeptidase B (1:100 enzyme to protein ratio; EMD Millipore) to cleave off the C-terminal residues such

as the His8 tag. Initial screens for crystallization of FLRT and FLRT-LPHN3 complex were carried out using 96-well format kits (Qiagen JCSG Core Suites 1-IV; Rigaku Wizard Crystallography Screens) on a Mosquito Crystal robot (TTP Labtech) at room temperature. Crystals of FLRT3 grew in D10 well of JCSG Core III suite (0.1M Tris pH7, 50% (v/v) PEG200) within 10days. Crystals were cryoprotected by transferring the crystals into mother liquor with 35 % glycerol. The best crystals diffracted to d_{min}=2.6 Å.

Similarly, crystallization trials for the FLRT/LPHN3 complex were obtained with 96-well screens. Initial crystal hit was observed in E7 well of Wizard Cubic LCP Block (Rigaku) containing 10% (w/v) PEG 3000, 100 mM MES pH6.0, 200 mM Lithium sulfate. To further optimize, 20 mg/ml protein complex in 10 mM HEPES pH7.2, 150 mM NaCl was mixed with equal volume of mother liquor, and equilibrated against 500 ul mother liquor in a 24-well format. Crystals grew to full size within 4 days and were cryoprotected with 20% glycerol. Many crystals displayed an intergrowth of two separate crystals in a variety of specific configurations, resulting in crystal twinning. The best crystals diffracted to d_{min}=2.6 Å.

Structure Determination and Refinement of FLRT3 and FLRT3/LPHN3 complex

Diffraction data was collected at Advanced Photon Source of the Argonne National Laboratories beamline 23-IBD and 19-BM. Data sets were processed using HKL2000. FLRT3 structure was solved by molecular replacement with Phaser-MR (Phenix) using a model of FLRT structure (PDB ID 4V2E). Similarly, FLRT3/LPHN3

structure was determined by molecular replacement using a homology model of the LPHN3 Olfactomedin domain based on the myocilin olfactomedin domain crystal structure (PDB ID 4WXQ). For both structures, refinement was performed in phenix.refine (Phenix) with nonscrystallographic symmetry (NCS) restraints. Olf structure in the complex was further refined using LPHN3 olf structure (PDB 5AFB). Since FLRT3/LPHN3 complex crystal displayed twinning, twin law of h, -k, -l was employed throughout the entire refinement process. Minor adjustments of the model were performed manually using COOT, followed by another round of refinement in Phenix. The final FLRT3/LPHN3 model contains four N-linked NAG carbohydrate moieties attached to each chain of the FLRT molecules in the FLRT3/LPHN3 complex structure. PISA program in the CCP4 package was used to analyze the structure such as calculation of the interface area and the hydrogen bonding interactions.

Flow cytometry

Cell culture

HEK293 cell line (ATCC; a generous gift from S. Koide lab) was cultured in Dulbecco's modified Eagle's medium (DMEM; Gibco) supplemented with 10% FBS (Gemini Bio-Products) at 37°C in 5% CO_2 humidified incubator. To seed for transfection cells were washed with PBS buffer and trypsinized (0.05% Trypsin-EDTA; Invitrogen). Cells were transiently transfected with Fugene 6 (PRE2693, Promega) at 60-70% confluence.

Sample preparation

HEK293 cells were transfected with 2 μg of DNA /well in 6-well plates using Fugene6. After 48 hrs of incubation, cells were detached with citric saline solution and washed with PBS and PBS+0.1% BSA (Bovine serum albumin, A3803, Sigma). The pellet was then stained with primary antibodies (in PBS+0.1% BSA) for 30 min (with rotation at room temperature), washed twice with PBS+0.1% BSA and incubated with secondary antibodies for another 30 min and washed twice again. Pellets were resuspended in PBS+0.1% BSA. Flow cytometry data were collected on Guava Easycyte flow cytometer (10000 events measured).

Cell labeling

To test LPHN3 WT and mutants expression, cells were stained with mouse anti-FLAG M2 antibodies, 1:1000 (F3165, "Sigma"). Fluorescence was determined by incubating with anti-mouse FITC, 1:100 (F0257, "Sigma"). For binding assays purified monomeric His-FLRT LRR was added to primary antibodies to final concentration 10 μM ; 100 nM precomplex of BTtrisNTA - NeutrAvidinDyLight 650 (NAV650) (84607, "Thermo Scientific") was used for fluorescent labeling. Otherwise cells were incubated with tetramerized His-FLRT LRR as a component of 100 nM precomplex HIS-FLRT3 LRR – NAV650 – BTtrisNTA. BTtrisNTA (biotinylated tris-nitrilotriacetic acid) – a reagent that effectively noncovalently biotinylates any poly-His-tagged protein - was generously provided by S. Koide lab.

To test FLRT3 WT and mutant expression, cells were stained with mouse anti c-Myc antibodies (9E10, "DSHB") 1:20 and anti-mouse FITC, 1:100. 100 nM

pretetramerized biotin-LPHN3 olf - NAV650 was used to test binding. Pretetramerization was done by mixing and incubating the reagents for 30 minutes. For Unc5 FLRT3 binding assays, cells transfected with Unc5B and Unc5D constructs as well as untransfected cells were stained with 100nM pretetramerized NAV650 – biotin-LPHN3 olf - His-FLRT3 LRR or NAV650 – biotin-LPHN3 olf - HIS-FLRT3-UF LRR.

Flow cytometry analysis

Sample analysis was performed using FlowJo Single Cell Analysis software and presented as histograms (for protein expression data) and dot plots (an overlay of two fluorescent signals which correspond for protein expression and binding). Also protein expression was presented as diagrams of mean fluorescence intensity for each sample. Gates were set to define a population of cells to show binding.

Bio-layer Interferometry Binding Measurement

Binding between FLRT3 and LPHN3 was performed using the BLITZ system (forteBio). FLRT3 or LPHN3 was then immobilized onto streptavidin sensors, and the unbound protein was washed off by HBS buffer (10mM HEPES pH7.2, 150mM NaCl). The sensor was then immersed into solutions containing immobilized protein's binding partner at various concentrations for 200s. Dissociation was carried out by immersion of sensor into HBS for 250s. Since LPHN3 failed to dissociate completely from the sensor, 3M $MgCl_2$ in HBS was used to regenerate the streptavidin sensor for 250s. The regeneration solution (3M MgCl2 in HBS) was

tested multiple rounds prior to the binding experiment to ensure it did not cause any undesired effects on the ligand or sensor chip.

Differential scanning fluorimetry

Differential scanning fluorimetry (DSF) assays were performed on a *CFX384™* (Bio-Rad). Prior to DSF assays, proteins were purified using Gel Filtration chromatography in a buffer containing 10mM HEPES pH 7.2 and 150mM NaCl. After gel filtration, samples were equilibrated to 25˚C. A 1:1000 dilution of SYPRO Orange (Invitrogen Molecular Probes) was used as a reporter dye to monitor the denaturing process of the proteins. Samples were assayed on a 384-well plate with final protein concentrations of 6 µM. The temperature was raised with a step of 0.5 °C per minute from 25 °C to 95 °C, collecting fluorescence readings at the end of each interval. Each sample was run in quadruplicate. Collected data was analyzed by *CFX-Manager™* from Bio-Rad. The negative temperature derivative of the fluorescence intensity was plotted as a function of temperature. The temperature corresponding to the minimum value of each curve reflects the midpoint of a two-state transition from folded to unfolded protein. This temperature was thus reported as the melting temperature of the protein (T_m).

Cell aggregation assays

FreeStyle HEK293 cells (Life Technologies) grown to a density of $1x10^6$ cells/mL in a 30mL volume were co-transfected with 30µg of either pCMV-Emerald or pCMV-dsRed and 30µg of the indicated construct using FreeStyle Max reagent (Life

Technologies). Cells were grown at 37°C/8%CO_2 with shaking at 125rpms. All cDNAs were driven by the CMV promoter. Transfected cells were mixed in a 1:1 ratio two days post-transfection and incubated for an additional 2 days. Live cells were imaged by dropping 100µL of cell suspension onto a glass slide (FisherBrand). Aggregation index was calculated as shown previously (Boucard et al. 2013. J. Cell Biol.).